Published in final edited form as:
Biomaterials. 2008 December ; 29(36): 4783–4791. doi:10.1016/j.biomaterials.2008.08.034.

Culture on Electrospun Polyurethane Scaffolds Decreases Atrial Natriuretic Peptide Expression by Cardiomyocytes *In Vitro*

Danielle N. Rockwood[1], **Robert E. Akins**[*,2], **Ian Parrag**[3], **Kimberly A. Woodhouse**[3], and **John F. Rabolt**[1]

1*Department of Materials Science and Engineering, University of Delaware 201 Dupont Hall, Newark, Delaware 19711*

2*NemoursBiomedical Research, A.I. duPont Hospital for Children 1600 Rockland Road, Wilmington, Delaware 19803*

3*Department of Chemical Engineering and Applied Chemistry, University of Toronto 200 College Street, Toronto, Ontario M5S 3E5, Canada*

Abstract

The function of the mammalian heart depends on the functional alignment of cardiomyocytes, and controlling cell alignment is an important consideration in biomaterial design for cardiac tissue engineering and research. The physical cues that guide functional cell alignment *in vitro* and the impact of substrate-imposed alignment on cell phenotype, however, are only partially understood. In this report, primary cardiac ventricular cells were grown on electrospun, biodegradable polyurethane (ES-PU) with either aligned or unaligned microfibers. ES-PU scaffolds supported high-density cultures, and cell subpopulations remained intact over two weeks in culture. ES-PU cultures contained electrically-coupled cardiomyocytes with connexin-43 localized to points of cell:cell contact. Multi-cellular organization correlated with microfiber orientation, and aligned materials yielded highly oriented cardiomyocyte groupings. Atrial natriuretic peptide, a molecular marker that has decreasing expression during ventricular cell maturation, was significantly lower in cultures grown on ES-PU scaffolds than in those grown on tissue culture polystyrene. Cells grown on aligned ES-PU had significantly lower steady state levels of ANP and constitutively released less ANP over time indicating that scaffold-imposed cell organization resulted in a shift in cell phenotype to a more mature state. We conclude that the physical organization of microfibers in ES-PU scaffolds impacts both multi-cellular architecture and cardiac cell phenotype *in vitro*.

Keywords

cardiac tissue engineering; electrospinning; biodegradable polyurethane; atrial natriuretic peptide (ANP); cardiomyocyte

*For correspondence: Robert E. Akins, Jr., Ph.D. Nemours Biomedical Research A. I. duPont Hospital for Children 1600 Rockland Road Wilmington, DE 19803 PH: (302) 651-6811 FAX: (302) 651-6897 Email: rakins@nemours.org.

Introduction

Cells in the mammalian heart communicate and contract in a highly directional manner, and cardiac ventricles contain ordered, multi-cellular structures comprising nearly parallel cardiomyocytes, which act in unison to provide efficient force production [1-3]. Controlling multicellular alignment is, therefore, a central goal in the design of biomaterials for cardiac tissue engineering, and understanding the effects of imposed alignment on cell phenotype is a critical area for research. In previous studies of tissue-level, multicellular organization *in vitro*, cardiac cell alignment has been induced using oriented scaffolds [4], patterned substrates [5,6], or mechanical conditioning of established cultures [7-10]. In seminal work on patterning, Simpson et al. demonstrated that cultured cardiomyocytes grown on aligned gel matrices adopt a morphologic phenotype typified by lateral cell alignment, elongated cell shape, and parallel myofibrillar organization, which are hallmarks of tissue-level organization [11]. In more recent work, McDevitt et al. demonstrated that cardiomyocytes could also be patterned using narrow strips of laminin, which caused cells to align in series and form intercalated disk-like structures located at end-to-end contact points similar those seen in native tissue [5,6]. The transmission of mechanical strain through the substratum to which cardiac cells are attached can also induce cellular alignment and subsequent morphologic adaptation consistent with tissue-level organization [7,9,10]. Significantly, although cells can be induced to align using matrix patterning or mechanical strategies, the organization of multi-cellular cardiac tissue structures seems to be principally driven by molecular responses to culture conditions [12]; unfortunately, the effects of induced cell alignment on cardiac cell molecular phenotype have been only partially described.

Atrial natriuretic peptide (ANP) is a critical marker for the molecular phenotype of cardiac muscle cells. During structural development of the heart, maturational changes in cardiac gene expression occur [13], including decreasing expression of ANP in the ventricle [14,15]. In the mature heart, ANP expression is largely restricted to atrial cells, which release the peptide from accumulated stores through a regulated mechanisms triggered by increased intermittent stretch during atrial filling. ANP is also produced in immature ventricular cells via a constitutive pathway, but production is down-regulated during normal maturation, and mature ventricular mycoytes only produce ANP under pathologic conditions associated with ventricular hypertrophy [14,15]. Since its production decreases with the structural maturation of the cardiac ventricle, ANP represents a useful marker for studying cardiac ventricular cell molecular phenotype.

To investigate the relationship between structural organization and ANP expression in cardiac ventricular cells *in vitro*, we prepared aligned and unaligned biodegradable polyurethane (PU) culture substrates by electrospinning. Electrospinning offers several advantages as a processing method for tissue engineered scaffolds including high surface area to volume ratios, formation of interconnected porous networks, and small diameter fibers that mimic the fibrous architecture of the extracellular matrix of soft tissue. In combination, these characteristics promote cell adhesion and migration and enable the transport of nutrients and waste throughout the scaffold [16-18]. Additionally, the electrospinning process can be tailored to create highly aligned scaffolds that can be used as templates for cell organization. In the present work, electrospun-PU (ES-PU) scaffolds were made from biodegradable, elastomeric material with tunable degradation properties [19] and used to culture primary neonatal rat heart cells. Cultures were prepared using both aligned and unaligned scaffolds and assayed for cell survival, maintenance of cell populations, and differences in markers of molecular phenotype, including ANP.

Methods

Polyurethane Synthesis

PU was synthesized using polycaprolactone diol with a molecular weight of 1250 (Aldrich, Milwaukee, WI), 2,6-diisocyanate methylcaproate (LDI; Kyowa Hakko Kogyo, Tokyo, Japan) and a L-phenylalanine-based diester chain extender (Toronto Research Chemicals, Toronto, ON, Canada) following the methods of Skarja and Woodhouse [20].

Electrospinning and Alignment

The PU was dissolved in dichloromethane (Sigma, St. Lo1uis, MO) at a concentration of 18% (w/v) as previously reported [19]. The electrospinning apparatus consisted of a variable speed syringe pump (Orion Sage, Thermo Scientific; Waltham, MA) and a high voltage power supply (Glassman Series ED, High Bridge, NJ). A glass syringe (Popper & Sons, New Hyde Park, NY) was equipped with a blunt-tipped needle (23 gauge, Hamilton, Reno, NV) and filled with the polymer solution. The syringe pump was set to a flow rate of 2.0 to 2.7 ml/hr to provide a continuous flow of solution to the tip, and +10 kV of voltage was applied to the needle. Isotropic fibrous mats were collected using a stationary collector whereas a rotating mandrel assembly was constructed to align the fibers for the anisotropic mats. A speed of 2000 RPM (10.6 m/sec) was used to align the fibers.

FE-SEM

Field emission-scanning electron microscope (FE-SEM) measurements were carried out on a JEOL JSM 7400F (Tokyo, Japan). Samples were coated with 10 Å of gold/palladium (Denton, Moorestown, NJ) prior to imaging. Images were obtained at a working distance of 8 millimeters at 1 kV. Fiber diameters for both aligned and isotropic mats were measured onboard JEOL software. Fiber orientation was determined from digital images using Image Pro® Plus software (Media Cybernetics, Silver Spring, MD). Briefly, on each image, a reference line was drawn, and the acute angle formed between the reference and the principal axis of individual fibers was recorded.

Mechanical Testing

Uniaxial tensile testing was performed using an Instron 4301 (Instron, Norwood, MA) with a crosshead speed of 13 mm/min and a 10 N load cell running at 50% capacity. Samples of ES-PU for tensile testing were prepared at 60-70 μm in thickness and cut into strips 3 cm long and 1 cm wide. Samples were stretched under ambient conditions until break in the preferred direction of fiber orientation. Force-elongation data were used to generate stress-strain curves; stress and strain at break and initial moduli were determined from the curves.

Cell Isolation and Culture

Neonatal rats (2-3 day old; Charles River Laboratories, Wilmington, MA) were anesthetized and euthanized under an IACUC-approved protocol. The ventricular portion of the heart was dissected, minced, and digested using a limited digestion with purified trypsin followed by complete digestion with collagenase using reagents from Worthington Biochemical Corporation (Freehold, NJ) as previously described [21]. Cell harvests were collected by centrifugation and filtered through 0.070 mm nylon mesh Nitex (Becton Dickinson, Franklin Lakes, NJ), and statically inoculated at 2×10^6 viable cells per 10 cm^2 of surface area using 6-well plates. Prior to inoculation, electrospun polyurethane (ES-PU) scaffolds and tissue culture polystyrene (TCPS) control wells were precoated with 100 μg/ml human fibronectin (FN, Becton Dickinson) for 18 hours followed by rinsing with Hank's Balanced Salt Solution (HBSS, Invitrogen, Carlsbad, CA). Cells were allowed to adhere for 24 hours prior to the first

feeding. Cultures were maintained in a serum-free medium (SFM) as previously reported [21].

Staining and Microscopy

To quantify the proportion of dead cells present in cultures, samples were rinsed with HBSS and stained for 20 minutes with a 1:500 dilution of ethidium homodimer-2 (1.29 mg/ml, EthH-2; Invitrogen) prior to fixation in 2% (w/v) paraformaldehyde (PFA, Electron Microscopy Sciences, Hatfield, PA) in Dulbecco's phosphate-buffered saline (PBS; pH 7.4; Mediatech, Inc., Manassas, VA) for 45 minutes. Cells were then permeabilized by the addition of Triton X-100 (Sigma) to 0.1% (v/v), rinsed in PBS, blocked with 3% (w/v) bovine serum albumin (BSA, Sigma, St. Louis, MO). Subsequent evaluations were carried out to determine live/dead cell ratio, the arrangement of sarcomeres, or the organization of gap junctions. For live/dead cell determination, cultures were counterstained with Hoechst 33258 (1 μg/ml, Sigma) and enumerated such that Eth-H2 positive nuclei indicated nuclei from dead cells out of total Hoechst 33258-positive nuclei. For sarcomeres, cells were stained with a primary antibody that recognizes myosin heavy chain (MyHC; clone A4.1025, Developmental Studies Hybridoma Bank, Iowa City, IA) by incubating for 2 hours in hybridoma medium diluted 1:1 with PBS followed by staining for 1 h with Texas Red conjugated anti-mouse IgG (Jackson ImmunoResearch, Media, PA), Hoechst 33258 (1 μg/ml, Sigma) to stain nuclei and Alexa Fluor 488-conjugated phalloidin (Invitrogen) to stain filamentous actin. For gap junctions, samples were incubated overnight in a 1:500 dilution of a monoclonal antibody against connexin43 (mouse anti-connexin-43 monoclonal, Chemicon, Temecula, CA) in PBS. Samples were then counter stained with Alexa Fluor 488-conjugated to anti-mouse IgG (Invitrogen), Hoechst 33258, and Alexa Fluor 546-conjugated phalloidin (Invitrogen). Images of fluorescently stained samples were acquired using an Evolution QEi, 12-bit, cooled CCD camera (Media Cybernetics) mounted to an Olympus model BX-60 epi-fluorescence microscope and operated using Image Pro® Plus software (Media Cybernetics). Alignment calculations and live/dead counts were accomplished using Image Pro® Plus.

Flow Cytometry

Cells for flow cytometry were collected via trypsinization (0.05% trypsin-EDTA, Invitrogen) of cultures. The collected cells were fixed in 2% PFA for 45 minutes, permeabilized with 0.1% (v/v) Triton X-100, and blocked with 3% BSA. Samples were stained with a primary antibody recognizing MyHC (A4.1025) and then labeled with a secondary antibody of Alexa Fluor 488-conjugated to anti-mouse IgG (Invitrogen). Samples were run through cell strainers (35μm, Becton Dickinson) and analyzed on a FACSCalibur flow cytometry instrument (Becton Dickinson). MyHC-positive cells were considered myocytes.

Gene Expression Analysis

Cells and tissue for real time, quantitative polymerase chain reaction (qPCR) were collected via trypsinization, rinsed with PBS, and stored in RNA-Later® at 4 °C for one week and then −20 °C, as per the manufacturer's recommendations (Ambion, Foster City, CA). RNA was prepared using QIAshredder and RNeasy® kits (Qiagen, Valencia, CA) following the protocols from the manufacturer. Potential DNA contamination of samples was eliminated by DNAse treatment (Turbo DNAse™, Ambion). The RNA was reverse transcribed using a RT^2 PCR Array First Strand Kit (SuperArray, Frederick, MD). QPCR was run on a MyiQ iCycler (BioRad, Hercules, CA) instrument using custom assays from SuperArray based on primers with proprietary sequences to detect glyceraldehyde-3-phosphate dehydrogenase (Gapdh), which is expressed by all cells, cardiac troponin I (Tnni3), which is specific to cardiomyocytes, myosin light polypeptide 3 (Myl3), which is specific to ventricular cardiomyocytes, and

natriuretic peptide precursor type A (Nppa), which encodes the ANP precursor that accumulates in atrial and immature ventricular cardiomyocytes.

Protein Quantification

To determine atrial natriuretic peptide (ANP) levels, an enzyme immunoassay (EIA, ANF (1-28) rat, host rabbit, high sensitivity, Bachem, San Carlos, CA) were performed on cellular extracts following the manufacturer's recommendations. The results indicated the total level of ANP, pro-ANP, and pre-pro-ANP in the sample. A bicinchoninic acid protein assay (Pierce Biotechnology, Rockford, IL) was performed to determine overall protein concentration in samples. The level of ANP as a function of total protein was compared between samples.

Statistical Analysis

Statistical analysis was carried out with SPSS Graduate Pack 15 (Chicago, IL) and Primer of Biostatistics (McGraw-Hill, Columbus, OH) software. Tests applied to individual datasets are indicated in the text.

Results

Cell Viability and Population Characteristics

To establish whether ES-PU scaffolds could support cardiac cell culture and to verify the stability of the primary cell populations over time, cell viability and flow cytometry assays were carried out. Viability was assessed using a fluorescent live/dead staining protocol in which the number of live and dead cells in random microscope fields was tabulated manually. The average percentage of live cells on isotropic ES-PU versus TCPS is shown over time in Figure 1. Overall, the percentage of live cells was somewhat lower on the ES-PU mats than on TCPS, but the percentage of viable cells on the PU was relatively stable over the first week of culture (85.5% on day 1; 83.7% on day 2; and 85.2% on day 7, respectively) but increased somewhat by day 14 (92.6%). In contrast, the percentage of live cells on the TCPS started at 93.6% after 24 hours, then decreased slightly to 89.5% and 88.3% on days 2 and 7, increasing to 95.3% at the final time point. Despite these changes, overall the data indicate that ES-PU supported viable cells to a level similar to that seen for TCPS without dramatic losses over the timeframe of the study.

Since primary cardiac cells comprise a mixed cell population predominated by non-proliferative cardiomyocytes and highly proliferative fibroblasts, we also determined whether the proportion of myocytes persisted over time in culture on ES-PU. Flow cytometry was used to determine the ratio of myocytes to non-myocytes. This ratio was measured for the initial cell isolate and at intervals throughout the length of the experiment. Cells staining positive for MyHC, which is only present in the cardiomyocyte component of these cultures, were categorized as myocytes while all remaining cells were considered non-myocytes. Figure 2 shows the average proportion of myocytes (n = 3) for each material at four time points. The initial cell isolate used in this experiment contained 36.3% myocytes indicating a relatively high proportion of potentially proliferative cells were present. The percentage of myocytes remained relatively unchanged after the cells had attached to the substrates such that by day 14, the percentage of myocytes was 31.8%, 28.5%, and 38.4% on aligned ES-PU, TCPS, and isotropic ES-PU, respectively. These numbers were not significantly different between time points or across different materials by Two Way ANOVA ($p>0.1$), anddespite the relatively low percentage of myocytes, all of these cultures beat throughout the duration of culture.

Alignment of polyurethane substrates and cultured cells

The first step in evaluating cellular alignment in our study was to create a template to guide the cells during seeding. This was done by fabricating isotropic (unaligned) and anisotropic (aligned) fibrous PU mats by electrospinning. Isotropic mats were prepared using a stationary, flat collector; whereas, aligned mats were collected on a rotating mandrel. The average fiber diameter was 1.8 ± 1.26 μm and 2.0 ± 1.92 μm for aligned and isotropic mats, respectively. As observed previously, [19] there was evidence of polymer bead formation and a large range in fiber diameters, from a few hundred nanometers to several microns that may have been caused by fiber splaying during the electrospinning process. Figure 3a-c shows FE-SEM images of both types of material and the relative fiber orientation in each. There was a clear difference in orientation of fibers within the isotropic and aligned mats that was quantified by assessing the variance of the fiber angle distributions (Figure 3c) using Levene's test for Homogeneity of Variance ($p \leq 0.01$).

Mechanical analysis of the different ES-PU mats indicated that the aligned scaffolds were considerably stiffer than the isotropic mats. The isotropic fibers had an elastic modulus of 13.5 MPa ± 1.2, ultimate tensile strain of 129% ± 26, and ultimate tensile stress of 1.53 MPa ± 0.06. In contrast, the aligned fibers showed an elastic modulus of 22.5 MPa ± 1.7, ultimate tensile strain of 70% ± 5, and an ultimate tensile stress of 2.84 MPa ± 0.08. Therefore, as expected, the aligned materials were stiffer and less extensible than the unaligned substrates.

Cells seeded onto aligned and isotropic mats appeared to adopt the underlying orientation of the materials by orienting to the long-axes of the ES-PU microfibers. As a result, multicellular groupings on the isotropic scaffolds appeared to be less organized than those on the aligned substrates, which appeared highly oriented relative to the material's axis. As expected (Figure 3d), the degree of alignment was significantly higher for the cells cultured on the aligned ES-PU. Significant differences were not seen between the alignment scores of isotropic fibers and that of cells grown on isotropic mats or between aligned fibers and cells grown on aligned mats.

Cell Morphology and Organization

The morphology and phenotype of the cultured cardiac cells were evaluated to determine whether cells on aligned versus unaligned substrates were able to establish oriented electrical communication and whether substrate patterning affected cell maturation status evinced by ANP production. **I**n Figure 4a-c, cytoskeletal MyHC (red), which is specific to myocytes, and filamentous actin (f-actin, green), which is present in all cell types but accumulate to a considerably higher level in cardiomyocytes due to the contractile apparatus [22], are shown in conjunction with the position of cell nuclei (blue). Cells on all of the substrates studied showed striated sarcomeres with organized f-actin and MyHC. In the TCPS and isotropic ES-PU cultures, the cells appeared relatively unaligned, and the contractile activity of cardiomyocytes on these substrates was not directionally organized. In contrast, cells seeded on aligned ES-PU microfibers were oriented and contractile in one principal direction with a more linear appearance, which is comparable to the organization of myocytes in ventricular tissue [22]. These observations were noted three days post-seeding and then throughout the duration of the experiments.

In vivo, the lateral alignment of cardiomyocyte contractile elements in ventricular tissue is accompanied by the organization of gap-junctional components in the intercalated discs found where myocytes join end-to-end [22]. Thus Cx43, which is the most prominent gap junction protein in ventricular tissue [23], demarks functional cell alignment; accordingly, we investigated the localization of Cx43 in our cultures. Figure 4d-f illustrates Cx43 distribution (red) relative to cell nuclei (blue), and f-actin (green). For all three substrata, Cx43 was found

around the cell periphery and did not specifically localize to end-to-end cardiomyocyte contacts although such structures were occasionally found (see black arrowhead in Figure 4f). These data indicate that cells were electrically coupled in all culture types but that gap junctions were not localized to intercalated disc-like structures at the ends of adjacent cells.

Molecular Phenotype

The molecular phenotype of the cells in our cultures was investigated by measuring the relative levels of mRNA for four genes via qPCR: Gapdh, Tnni3, Myl3, and Nppa. Gapdh levels, which are commonly employed for normalizing gene expression data [24], were used as an indicator of total cell transcription activity. Tnni3, which is the troponin I isoform expressed in atrial and ventricular cardiomyocytes, and Myl3, which is the ventricular myocyte specific isoform of essential myosin light chain [25,26], were used to indicate total cardiomyocyte and ventricular cardiomyocyte subpopulations, respectively. Nppa, which is preferentially expressed in atrial, immature ventricular, and hypertrophic ventricular tissue but not in mature, healthy ventricular tissue [27-29], was used as an indicator of cardiomyocyte phenotype.

As shown in Figure 5, mRNA levels for Gapdh, Tnni3, and Myl3 were not significantly different across treatment groups indicating that the total cell transcriptional activity, cardiomyocyte-specific transcriptional activity, and ventricle-specific transcription were similar in TCPS and ES-PU cultures. Nppa, on the other hand, was relatively up-regulated in cells cultured on TCPS such that steady state Nppa-mRNA levels were elevated from day one onward. These data suggest that microfibrous ES-PU substrates supported cardiac cell populations that were similar to those grown on TCPS in terms of molecular phenotype but that culture on ES-PU resulted in an alteration of cardiomyocyte maturational status.

To further investigate Nppa expression, levels of immunoreactive atrial natriuretic peptide (ANP), which is encoded by the Nppa gene and comprises pre-pro-ANP, pro-ANP and ANP itself, were determined in the cells and medium of 7 day old cultures by EIA. As shown in Figure 6, cells grown on TCPS contained the highest level of ANP (1.584 ± 0.116 ng per mg of extracted cellular protein). Cells on isotropic ES-PU had slightly lower but similar levels of ANP (1.481 ± 0.174 ng/mg); however, cells grown on aligned ES-PU had significantly lower ANP content (0.407 ± 0.114 ng/mg). For reference, the ANP content of adult (0.68 ng/mg) and neonatal (3.39 ng/mg) ventricular tissue were also determined. Levels of ANP released into the medium during the 48 hours leading up to culture termination (i.e. between days 5 and 7) were also quantified. Cells grown on TCPS, isotropic ES-PU, and aligned ES-PU all released significantly different amounts of ANP (229.94 ± 16.80, 79.36 ± 28.87, and 22.35 ± 2.30 ng in 48 hours, respectively). These data suggest that compared to TCPS, culturing primary cardiac cells on aligned ES-PU induced cardiomyocytes to produce, store, and release less ANP, which is indicative of a more mature phenotype, with cells cultured on isotropic ES-PU adopting an intermediate phenotype between TCPS and aligned ES-PU.

Discussion

We have found that primary cardiomyocytes can be induced to align when cultured on microfibrous ES-PU substrates and that culture on ES-PU results in an alteration of cell phenotype such that aligned cultures produce less ANP than non-aligned cultures. Previous studies have shown that cells can be aligned by patterning cues from the underlying substrate [4-6] or by imposed mechanical loads subsequent to attachment [7-10]; however, the effects of alignment strategies on the molecular phenotype of component cells are not well understood. Our observations are consistent with a more mature phenotype being adopted by cells grown on aligned microfibrous ES-PU thus linking biomaterial patterning with cell phenotype.

A shift in the maturational phenotype of cultured cardiac cells is supported by assays of steady state mRNA levels. Gapdh mRNA levels indicated that samples contained similar amounts of overall cellular material. The Tnni3 and Myl3 data indicated that contributions from ventricular cardiomyocytes were essentially the same across samples, and in combination with the Gapdh data, that there were no significant differences in the hypertrophic status of cells cultured on the different substrates. This latter interpretation is further supported by the flow cytometric data, which indicated that the proportion of cardiomyocytes in the cell population of each culture type was essentially the same. Thus, the decreased levels of Nppa seen in cultures grown on aligned ES-PU are not likely to be accounted for by broad differences in cellular content or transcriptional activity or by more specific differences in cardiomyocyte hypertrophic status.

The isotropic and aligned ES-PU mats used in this study provided substrata that could be tailored to provide two different cellular environments. The difference between these two substrates was quantified, as shown in Figure 3, and the aligned fibers were found to be significantly more oriented than the isotropic mat. When cells were seeded on these materials, they aligned along the axes of the local fibers, and the organization of cells in culture mimicked the underlying organization of the fibrous mats. This result suggests the ES-PU microfibers can be used to pattern multi-cellular organization.

In addition, we observed through viability assays that ES-PU scaffolds supported primary cardiomyocyte cultures over time. In comparison to TCPS, there was a higher proportion of dead to live cells on the ES-PU even at early time points, suggesting that the dead cells present in the initial isolate may have been trapped in the fibrous ES-PU matrix during cell inoculation. Dead cells are typically washed away from culture dishes by medium exchanges, and it seems likely that it would be easier to wash TCPS surfaces than ES-PU fibers, which would be expected to entrap material seeded on it. As shown in Figure 1, there was a general trend of this type in our cultures. Critically, though, the number of dead cells did not increase over time in either TCPS or ES-PU cultures indicating that ES-PU supports cardiomyocyte cultures to a degree similar to that seen on TCPS. Additionally, the morphology of the cells, as shown by immunofluorescence, demonstrates the survival of cardiac cells on ES-PU membranes. Myocytes with striated myosin heavy chain interlaced with filamentous actin were found on both types of ES-PU mats and on TCPS (Figure 4). This staining pattern is indicative of healthy, contractile myocytes, and spontaneous contractility was evident on TCPS and ES-PU mats.

It is important to note that solid organs like the heart comprise of mixtures of cells and that the present experiments were carried out using a mixed cell population representative of what is found in native heart tissue [30-32]. Although cardiomyocytes are generally nonproliferative [23], proliferation of other subpopulations of heart cells can result in dramatic changes in relative cell contributions. Differential proliferation is, therefore, a critical concern in the interpretation of primary culture experiments. Accordingly, we prepared our cultures to limit overall proliferation: cells were inoculated at high density to elicit contact inhibition of cell division and a serum-free medium was used to reduce serum-induced proliferation. To verify that cell populations were uniform, we used flow cytometry to assess potential changes in the cardiomyocyte versus non-cardiomyocyte subpopulations through fourteen days in culture and found that the overall ratio of myocytes to non-myocytes remained relatively unchanged over the course of our experiments (see Figure 2). In combination with the live/dead assay results and immunostaining observations, these data indicate that cardiomyocytes survived two weeks in culture and that cell proliferation was severely restricted with no significant differences found between TCPS and ES-PU substrates. These data are further corroborated by the molecular analyses, especially Gapdh, Tnni3, which showed no differences across samples, and immunostaining observations.

Immunostaining results showed that multi-cellular organization differed among cultures on different substrata. In particular, neighboring cells cultured on TCPS and isotropic ES-PU extended in different directions; whereas, cells grown on aligned ES-PU ran in parallel following the template of the fibrous matrix, an organization that is similar to what is seen in native ventricular tissue [1]. To beat synchronously, cardiomyocytes must be electrically coupled through gap junctions. As seen in Figure 4, the gap junctional protein Cx43 in our cultures was distributed throughout the cells and not restricted to intercalated disks at end-to-end contacts. Interestingly, McDevitt et al. [5,6] found a similar Cx43 distribution when cells were seeded on unpatterned substrates but found that Cx43 localized to intercalated disks in cells restricted to 15-30 μm patterned lanes of laminin (spaced 20 μm apart), a geometry that limited side-to-side contact between cells and emphasized end-to-end contact of cells in series. In our experiments, cells were laterally aligned but formed side-to-side contacts, and Cx43 was seen at contacts between cells organized in series and in parallel. Thus, it appears that the presence of cell-to-cell contacts may influence the distribution of gap junctions on patterned materials, and to drive Cx43 organization to intercalated disks, it may be necessary to emphasize longitudinal contacts early in the culture but allow lateral contacts to form as cells grow later in culture. It should also be noted that mechanical load plays a key role in the determination of multi-cellular organization. In particular, mechanical load placed on cardiomyocytes *in vitro* results in morphological changes similar to those during heart development *in vivo* [7,9,33,34]. The application of controlled substrate patterning in conjunction with cyclic stretch may, therefore, allow engineers to drive cells to desirable architectures and cell phenotypes.

The molecular phenotype of cells was assessed by measuring the steady-state levels of mRNA expressed for Gapdh, Tnni3, Myl3, and Nppa. Gapdh was used as a ubiquitous marker for expression, Tnni3 as a marker for cardiac muscle cells generally, Myl3 as a marker for ventricular cardiomyocytes specifically, and Nppa as a marker for ventricular cardiomyocyte maturation. The amount of Gapdh, Tnni3, and Myl3 in the total mRNA isolates was not significantly different between samples, supporting the conclusion that the cell populations did not differ across substrata. Interestingly, given the cell and molecular data we obtained, differences in Nppa expression could not easily be accounted for by differences in RNA yield/integrity (Gapdh), the proportion of cardiomyocytes present (Tnni3), or the phenotypic conversion of the neonatal ventricular myocytes to an atrial phenotype (Myl3). Thus, the shift in ANP expression in cultures grown on ES-PU appears to be most likely accounted for by a shift in cardiomyocyte maturational status.

To further characterize the regulation of Nppa, ANP was measured at the protein level. Nppa is the mRNA precursor to ANP, which is an endocrine factor that modulates blood volume [14,15]. In adults, ANP is primarily synthesized in the cardiac atria, which release ANP in response to increased filling volume [15,22,35]. ANP also appears to play a role in cardiac development [29], where it may act as an inhibitor of hypertrophic growth [36] or a modulator of apoptosis [37]. Perhaps associated with this latter function, ventricular myocytes produce ANP during development, but as ventricular tissue matures perinatally, ANP production falls to levels <1% that seen in atria [15]. Elevated ANP production, therefore, is suggestive of either an atrial or immature ventricular cardiomyocyte phenotype. Since the cells used in our study were of ventricular origin and uniformly expressed Myl3, ANP levels are best interpreted as indicating maturational status.

The processing of Nppa into ANP has been well studied [14,15], and although detailed mechanisms remain unelucidated, the general mechanisms by which ANP is released from ventricular and atrial tissues are known to differ. In both cell types, Nppa mRNA is initially translated into a 152-amino acid pre-pro-ANP which is subsequently cleaved to form the 126-amino acid pro-ANP. Atrial myocytes subsequently release ANP through a regulated pathway

wherein the prohormone is stored in granules for rapid release after increased stretch. In contrast, ventricular cardiomyocytes secrete ANP via a constitutive pathway in which ANP is released shortly after synthesis and proANP is generally not stored in granules [28,38]. Importantly, immature cardiac ventricular tissue actively produces ANP and, therefore, has higher steady state levels of Nppa mRNA and immunoreactive ANP and also constitutively releases more ANP over time than mature ventricular tissue.

Detailed mechanisms to explain the observed shift in ANP metabolism are somewhat difficult to ascertain as details of ANP regulation remain unclear, especially how the expression of the Nppa gene, which encodes the ANP precursor, is controlled and how intracellular ANP levels are modulated [14,15]. Possible explanations for the observed effect include (i) biomechanical influences and (ii) alteration of cell:cell interactions. Biomechanical influences play a significant role in modulating ANP production *in vivo*. Specifically, ANP release is elevated by increased atrial or ventricular stretch during diastole (i.e. pre-load) and under hypertrophic conditions [15,36], which are associated with increased resistance during systole (i.e., afterload). In our experiments, however, there is no stretching/preloading of cells, and our data indicate that there were no significant differences in the hypertrophic status of cells cultured on the different substrata. In addition, the aligned scaffolds were stiffer than isotropic scaffolds suggesting that cardiomyocytes grown on aligned ES-PU should actually have higher ANP production than cells grown on the isotropic material if resistance to contraction were the major determinant of ANP production.Thus, although a role for biomechanical influences in regulating ANP cannot be ruled out, the biomechanical conditions associated with the modulation of ANP *in vivo* (stretch/preload or hypertrophy/afterload) are apparently not responsible for the alteration of ANP levels we observe. Cellular interactions offer an alternative explanation. Variations in substrate topography and texture are known to affect cell:cell interactions, and the Notch signaling pathway, which is triggered by particular cell:cell contacts, is known to modulate ANP expression [39,40]. Thus, differences in the quantity and quality of cell:cell interactions on different substrates may account for differences in ANP production.

In our study, cultures grown on TCPS or on isotropic ES-PU had significantly higher steady-state ANP levels than those found in cells grown on aligned ES-PU (Figure 6). In addition, cells grown on the different substrata showed a decreasing progression of ANP release with TCPS cultures exhibiting the highest constitutive production of ANP, followed by isotropic ES-PU, and finally aligned ES-PU. Viewed in conjunction with the mRNA data, these results indicate that culture on ES-PU influenced cells to adopt a more mature phenotype and that the aligned ES-PU provided the most mature cells. Interestingly, the isotropic ES-PU showed lower Nppa mRNA and reduced ANP release compared to the TCPS samples despite the observation of similar steady-state peptide levels. Thus, cells on isotropic ES-PU adopted a somewhat intermediate phenotype where the rate of ANP expression and the rate of pro-ANP to ANP conversion by corin-like proteases may both be attenuated relative to cells on TCPS but potentiated relative to cells on aligned ES-PU. Taken together, these results indicate that aligning cultured, primary, cardiac cells using physical cues from a biomaterial scaffold cannot only induce organizational changes relative to unaligned materials, but can also induce phenotypic changes in the component myocytes.

Conclusions

We demonstrate that biodegradable polyurethane can be electrospun into isotropic and aligned microfibrous templates capable of supporting primary cardiac cell culture in serum-free medium. Since PU-based materials are non-toxic and erode slowly over time, aligned ES-PU may provide useful scaffolds for engineering anisotropic cell sheets that are organized like native cardiac tissue. We also found that primary cardiac cells attain aspects of a mature

phenotype when grown on aligned and isotropic ES-PU. Specifically, immunoreactive ANP levels were significantly reduced in cultures grown on aligned ES-PU compared to otherwise identical cells grown on unaligned ES-PU or on TCPS controls. These results indicate that the physical patterning of ES-PU scaffolds affected both cell organization and cell phenotype.

Acknowledgements

The authors would like to thank Therese McLaughlin for help with cell culture, Frank Kriss and Dr. Chao Ni for assistance in electron microscopy, and Melissa Rhodes, Steve Beard, Alfred Lance and Dave Cowgill for help in manufacturing the mandrel used for aligning the fibers during electrospinning. In addition, the authors greatly appreciate the help of Dr. Chuanzhao Li and Robert Long with flow cytometry data collection. This work was funded through NSF (NIRT and DMR - 0315461 to JFR), the National Center for Research Resources at NIH (RPG# 1P20-RR020173-01 to REA), the Nemours Foundation (REA), the Canadian Institutes for Health Research (KAW), and the Natural Science and Engineering Research Council - Canada (KAW).

References

1. Schulte RE, Sachse FB, Werner CD, Dossel O. Rule Based Assignment of Myocardial Sheet Orientation. Biomed Tech (Berl) 2000;45(2):97–102.
2. LeGrice IJ, Smaill BH, Chai LZ, Edgar SG, Gavin JB, Hunter PJ. Laminar structure of the heart: Ventricular myocyte arrangement of connective tissue architecture in the dog. Am J Physiol 1995;269:H571. [PubMed: 7653621]
3. Hooks DA, Trew ML, Caldwell BJ, Sands GB, LeGrice IJ, Smaill BH. Laminar Arrangement of Ventricular Myocytes Influences Electrical Behavior of the Heart. Circ Res 2007;101:e103–e12. [PubMed: 17947797]
4. Riboldi SA, Sadr N, Pigini L, Neuenschwander P, Siomonet M, Mognol P, et al. Skeletal myogenesis on highly orientated microfibrous polyesterurethane scaffolds. J Biomed Mater Res Part A 2008;84A (4):1094–101.
5. McDevitt TC, Angello JC, Whitney ML, Reinecke H, Hauschka SD, Murry CE, et al. In vitro generation of differentiated cardiac myofibers on micropatterned laminin surfaces. J Biomed Mater Res 2002;60 (3):472–9. [PubMed: 11920672]
6. McDevitt TC, Woodhouse KA, Hauschka SD, Murry CE, Stayton PS. Spatially organized layers of cardiomyocytes on biodegradable polyurethane films for myocardial repair. J Biomed Mater Res 2003;66A(3):586–95.
7. Vandenburgh HH, Solerssi R, Shansky J, Adams JW, Henderson SA. Mechanical stimulation of organogenic cardiomyocyte growth in vitro. American Journal of Physiology-Cell Physiology 1996;39 (5):C1284–C92.
8. Carrier RL, Rupnick M, Langer R, Schoen FJ, Freed LE, Vunjak-Novakovic G. Perfusion improves tissue architecture of engineered cardiac muscle. Tissue Eng 2002;8(2):175–88. [PubMed: 12031108]
9. Zimmermann W-H, Schneiderbanger K, Schubert P, Didie M, Munzel F, Heubach JF, et al. Tissue Engineering of a Differentiated Cardiac Muscle Construct. Circ Res 2002;90(2):223–30. [PubMed: 11834716]
10. Fink C, Ergun S, Kralisch D, Remmers UTE, Weil J, Eschenhagen T. Chronic stretch of engineered heart tissue induces hypertrophy and functional improvement. FASEB J 2000;14(5):669–79. [PubMed: 10744624]
11. Simpson DG, Terracio L, Terracio M, Price RL, Turner DC, Borg TK. Modulation of cardiac myocyte phenotype in vitro by the composition and orientation of the extracellular matrix. J Cell Physiol 1994;161(1):89–105. [PubMed: 7929612]
12. Baudino TA, McFadden A, Fix C, Hastings J, Price R, Borg TK. Cell patterning: interaction of cardiac myocytes and fibroblasts in three-dimensional culture. Microscopy and microanalysis 2008;14(2): 117–25. [PubMed: 18312716]
13. Nemer M. Genetic insights into normal and abnormal heart development. Cardiovascular Pathology 2008;17(1):48–54. [PubMed: 18160060]
14. McGrath MF, de Bold AJ. Determinants of natriuretic peptide gene expression. Peptides 2005;26(6): 933–43. [PubMed: 15911063]

15. Pandey KN. Biology of natriuretic peptides and their receptors. Peptides 2005;26(6):901–32. [PubMed: 15911062]
16. Lu L, Mikos AG. The Importance of New Processing in Tissue Engineering. MRS Bulletin 1996;31 (11):28–32. [PubMed: 11541498]
17. Zong X, Bien H, Chung C-Y, Yin L, Fang D, Hsiao BS, et al. Electrospun fine-textured scaffolds for heart tissue constructs. Biomaterials 2005;26(26):5330–8. [PubMed: 15814131]
18. Riboldi SA, Sampaolesi M, Neuenschwander P, Cossu G, Mantero S. Electrospun degradable polyesterurethane membranes: potential scaffolds for skeletal muscle tissue engineering. Biomaterials 2005;26(22):4606–15. [PubMed: 15722130]
19. Rockwood DN, Woodhouse KA, Fromstein JD, Chase DB, Rabolt JF. Characterization of biodegradable polyurethane microfibers for tissue engineering. Journal of Biomaterials Science-Polymer Edition 2007;18(6):743–58. [PubMed: 17623555]
20. Skarja GA, Woodhouse KA. Synthesis and Characterization of degradable polyurethane elastomers containing an amino acid-based chain extender. J Biomater Sci Polymer Edn 1998;9(3):271–95.
21. Akins RE, Gratton K, Quezada E, Rutter H, Tsuda T, Soteropoulos P. Gene expression profile of bioreactor-cultured cardiac cells: Activation of morphogenetic pathways for tissue engineering. DNA Cell Biol 2007;26(6):425–34. [PubMed: 17570766]
22. Opie, LH. Heart Physiology: From Cell to Circulation. Vol. 4th Edition ed.. Lippincott Williams & Wilkins; Philadelphia: 2004.
23. Reinecke H, MacDonald GH, Hauschka SD, Murry C. Electromechanical Coupling between Skeletal and Cardiac Muscle: Implications for Infarct Repair. J Cell Biol 2000;149(3):731–40. [PubMed: 10791985]
24. Barber RD, Harmer DW, Coleman RA, Clark BJ. GAPDH as a housekeeping gene: analysis of GAPDH mRNA expression in a panel of 72 human tissues. Physiol Genomics 2005;21(3):389–95. [PubMed: 15769908]
25. Guenet JL, SimonChazottes D, Gravel M, Hastings KEM, Schiaffino S. Cardiac and skeletal muscle troponin I isoforms are encoded by a dispersed gene family on mouse Chromosomes 1 and 7. Mamm Genome 1996;7(1):13–5. [PubMed: 8903721]
26. Barth AS, Merk S, Arnoldi E, Zwermann L, Kloos P, Gebauer M, et al. Functional profiling of human atrial and ventricular gene expression. Pflugers Archiv-European Journal of Physiology 2005;450 (4):201–8. [PubMed: 15877233]
27. Claycomb WC. Atrial-Natriuretic-Factor Messenger-Rna Is Developmentally Regulated in Heart Ventricles and Actively Expressed in Cultured Ventricular Cardiac-Muscle Cells of Rat and Human. Biochem J 1988;255(2):617–20. [PubMed: 2974280]
28. Bloch KD, Seidman JG, Naftilan JD, Fallon JT, Seidman CE. Neonatal Atria and Ventricles Secrete Atrial Natriuretic Factor via Tissue-Specific Secretory Pathways. Cell 1986;47:695–702. [PubMed: 2946416]
29. Cameron VA, Ellmers LJ. Minireview: Natriuretic Peptides during Development of the Fetal Heart and Circulation. Endocrinology 2003;144(6):2191–4. [PubMed: 12746273]
30. Harding SE, Davies CH, Wynne DG, Poolewilson PA. Contractile Function and Response to Agonists in Myocytes from Failing Human Heart. Eur Heart J 1994;15:35–6. [PubMed: 7713111]
31. Sperelakis N. Cultured Heart Cell Reaggregate Model for Studying Cardiac Toxicology. Environ Health Perspect 1978;26:243–67. [PubMed: 214299]
32. Wollenberger A. Isolated Heart-Cells as a Model of the Myocardium. Basic Res Cardiol 1985;80:9–13. [PubMed: 3904721]
33. Yamane M, Matsuda T, Ito T, Fujio Y, Takahashi K, Azuma J. Rac1 activity is required for cardiac myocyte alignment in response to mechanical stress. Biochem Biophys Res Commun 2007;353:1023–7. [PubMed: 17207463]
34. Matsuda T, Takahashi K, Nariai T, Ito T, Takatani T, Fujio Y, et al. N-cadherin-mediated cell adhesion determines the plasticity for cell alignment in response to mechanical stretch in cultured cardiomyocytes. Biochem Biophys Res Commun 2005;326(1):228–32. [PubMed: 15567175]
35. de Bold AJ, Borenstein HB, Veress AT, Sonnenberg H. A rapid and potent natriuretic response to intravenous injection of atrial myocardial extract in rats. Life Sci 1981;28(1):89–94. [PubMed: 7219045]

36. Horio T, Nishikimi T, Yoshihara F, Matsuo H, Takishita S, Kangawa K. Inhibitory Regulation of Hypertrophy by Endogenous Atrial Natriuretic Peptide in Cultured Cardiac Myocytes. Hypertension 2000;35(1):19–24. [PubMed: 10642269]

37. Wu C-F, Bishopric NH, Pratt RE. Atrial Natriuretic Peptide Induces Apoptosis in Neonatal Rat Cardiac Myocytes. J Biol Chem 1997;272(23):14860–6. [PubMed: 9169455]

38. Irons CE, Sei CA, Glembotski CC. Regulated secretion of atrial natriuretic factor from cultured ventricular myocytes. Am J Physiol Heart Circ Physiol 1993;264(1):H282–5.

39. Xin M, Small EM, van Rooij E, Qi X, Richardson JA, Srivastava D, et al. Essential roles of the bHLH transcription factor Hrt2 in repression of atrial gene expression and maintenance of postnatal cardiac function. Proceedings of the National Academy of Sciences 2007;104(19):7975–80.

40. Koibuchi N, Chin MT. CHF1/Hey2 plays a pivotal role in left ventricular maturation through suppression of ectopic atrial gene expression. Circ Res 2007;100(6):850–5. [PubMed: 17332425]

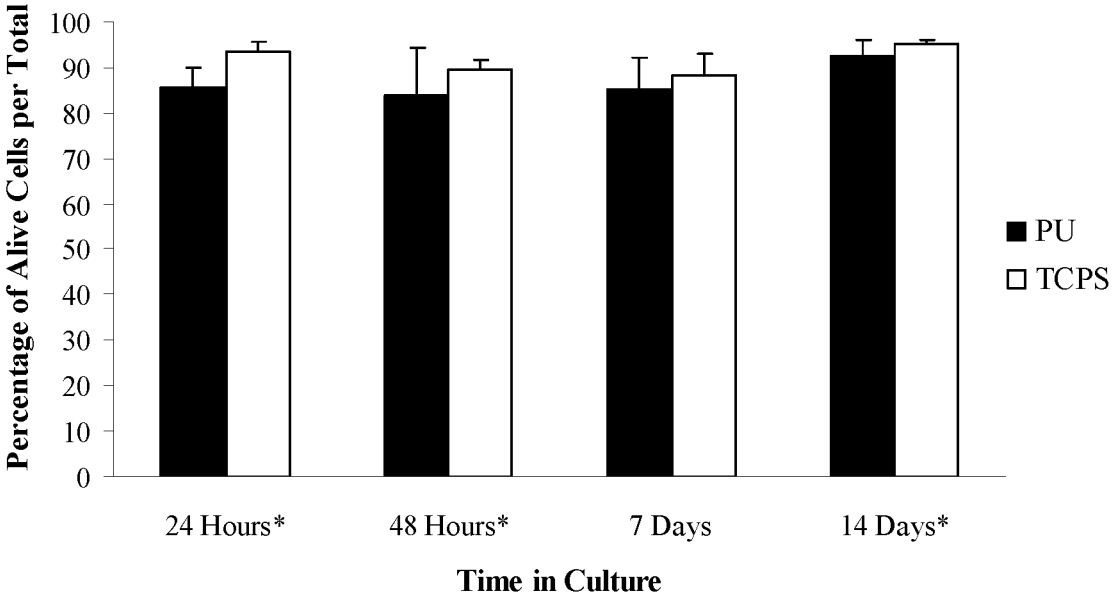

Figure 1. Cell survival during culture

Live and dead cells were enumerated in cultures grown on ES-PU fibers and on TCPS. Although the proportion of live cells was similar in all samples, statistically significant differences were found between ES-PU and TCPS samples taken on days 1, 2, and 14 by Chi square test ($p \leq 0.05$). Data shown are mean ± S.D., n = 3.

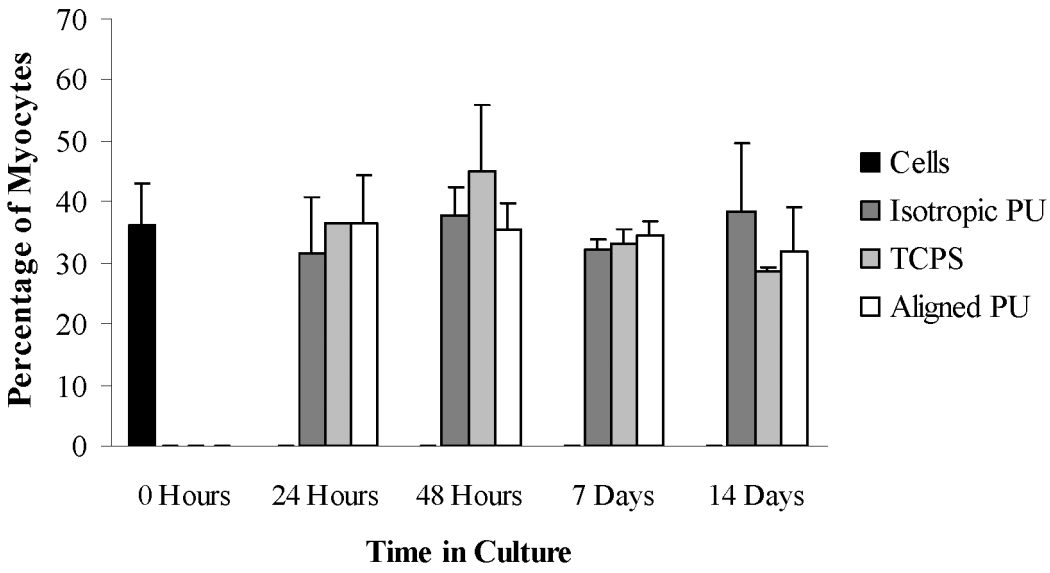

Figure 2. Flow cytometry

Analysis of cell populations from the initial isolate and samples collected after 24 hours, 48 hours, 7 days, and 14 days in culture on TCPS, isotropic, and aligned PU. Data are mean ± SD, n=3. No significant differences were found by 2 Way ANOVA.

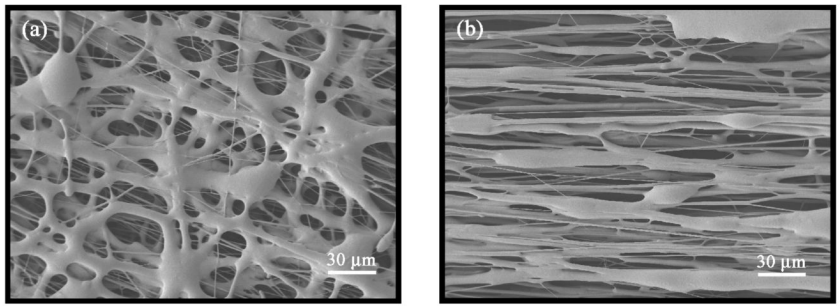

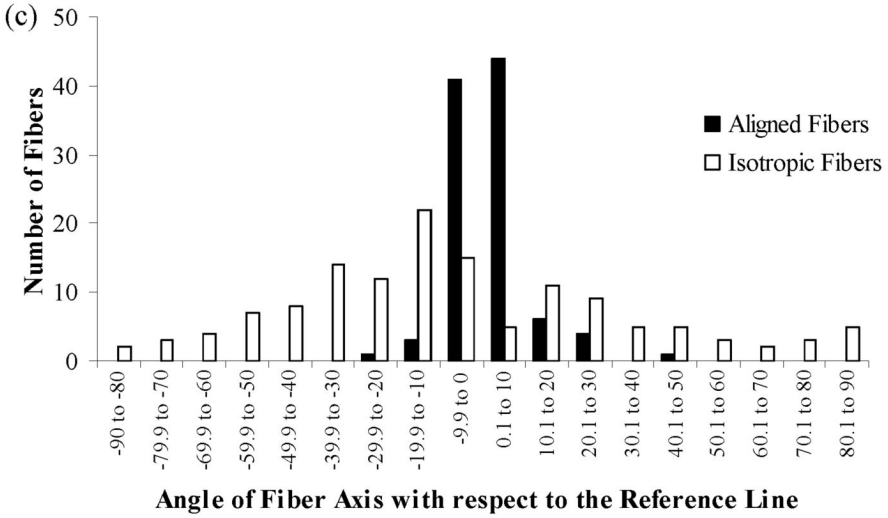

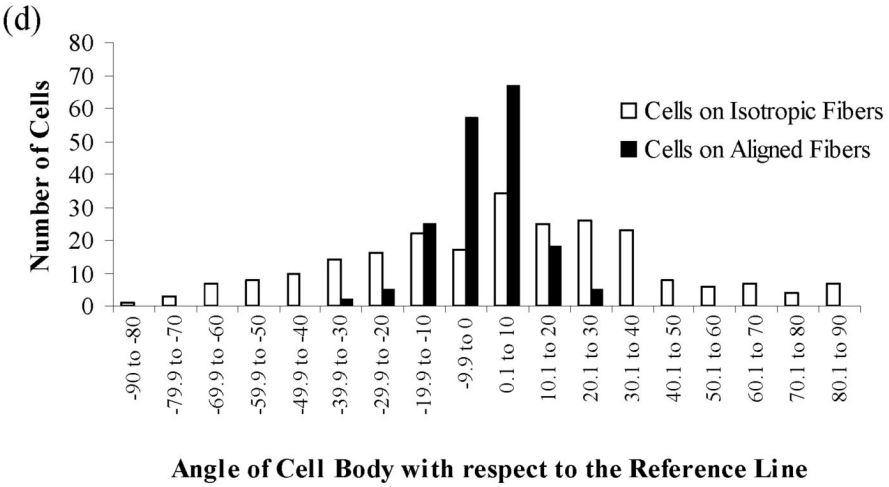

(e)

	Aligned Fibers	*Isotropic Cells*	*Aligned Cells*
Isotropic Fibers	0.001*	0.467	0.001*
Aligned Fibers	X	0.001*	0.019
Isotropic Cells	X	X	0.001*

Figure 3. Determination of fiber and cell alignment in ES-PU cultures

Isotropic (a) and aligned fibrous mats (b) were used as templates for cellular organization. The alignment of the (c) fibers and (d) cells was quantified with respect to a reference line and is represented as the angle from the reference line ± 90°. (e) Statistical analysis of fiber and cell alignment was done via a Levene's tests for homogeneity of variance and subsequent tests. Here the p-values are shown and significant differences ($p \leq 0.01$) are indicated by an asterisk.

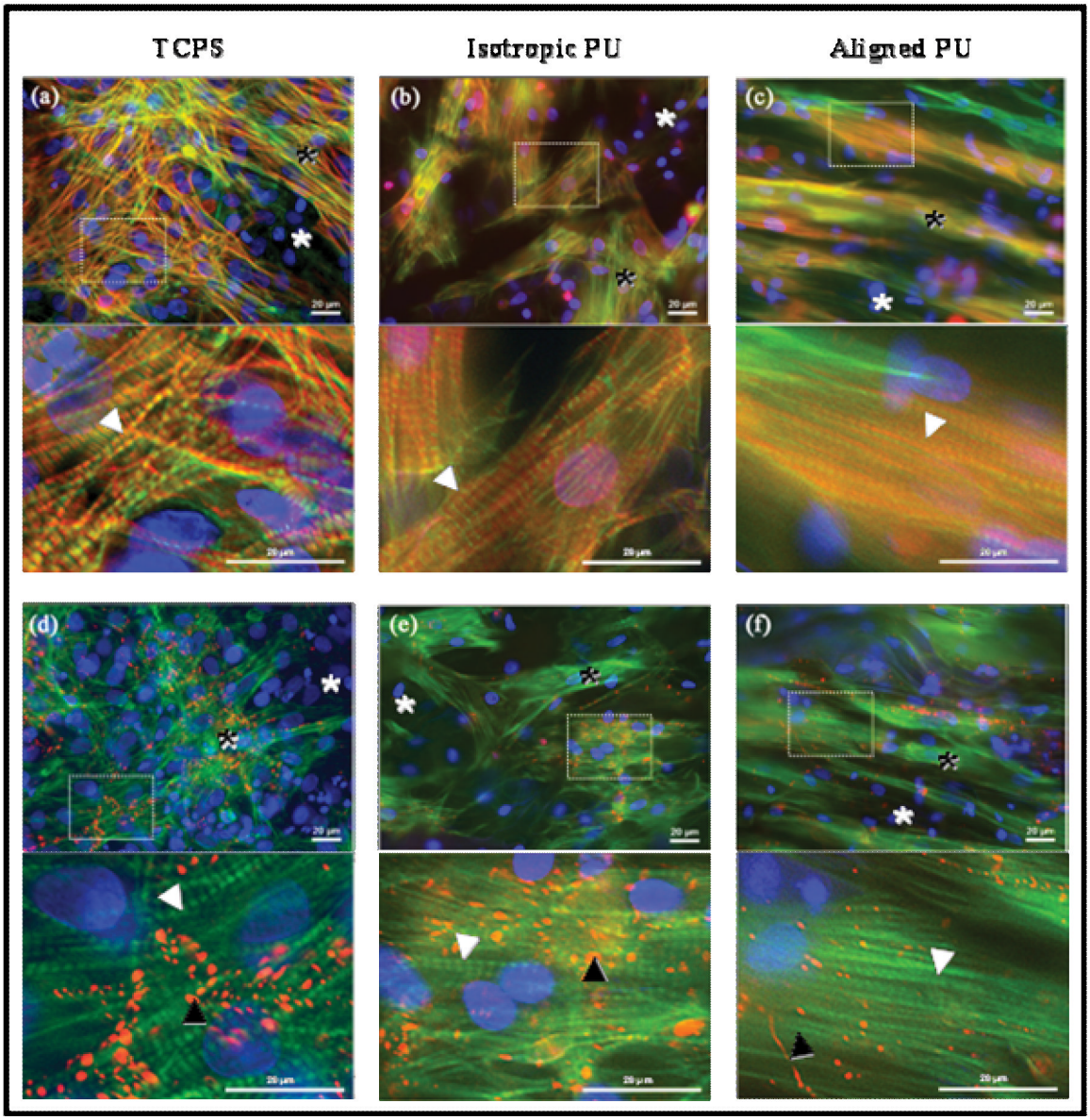

Figure 4. Cellular organization

Samples were stained for f-actin (green), nuclei (blue), and either muscle-specific myosin heavy chain (red in panels a, b, and c) or gap-junction-specific connexin-43 (red in d, e, and f) to visualize cellular structures. The top image in each pair shows a merged, three-color fluorescence micrograph obtained at low magnification to show typical staining patterns of cells cultured on TCPS (a, d), isotropic ES-PU microfibers, and aligned ES-PU microfibers. The bottom image in each pair shows a 4x zoomed view of the region indicated by the rectangle in each upper image to allow visualization of sub-cellular structures. Cells seeded on TCPS (a, d) and isotropic ES-PU fibers (b, e) were substantially less oriented than those grown on aligned ES-PU microfibers (c, f). In all cases, muscle cells (black asterisks) and non-muscle cells (white asterisks) were present. Striations from organized sarcomeric proteins in cardiomyocytes (white arrow heads) were prevalent in all samples; however, these were generally more difficult to resolve in ES-PU samples due to apparent lensing effects from the underlying biomaterial.

Cx-43 staining of gap junctions was also prevalent (black arrowheads). Scale bars represent 20 μm.

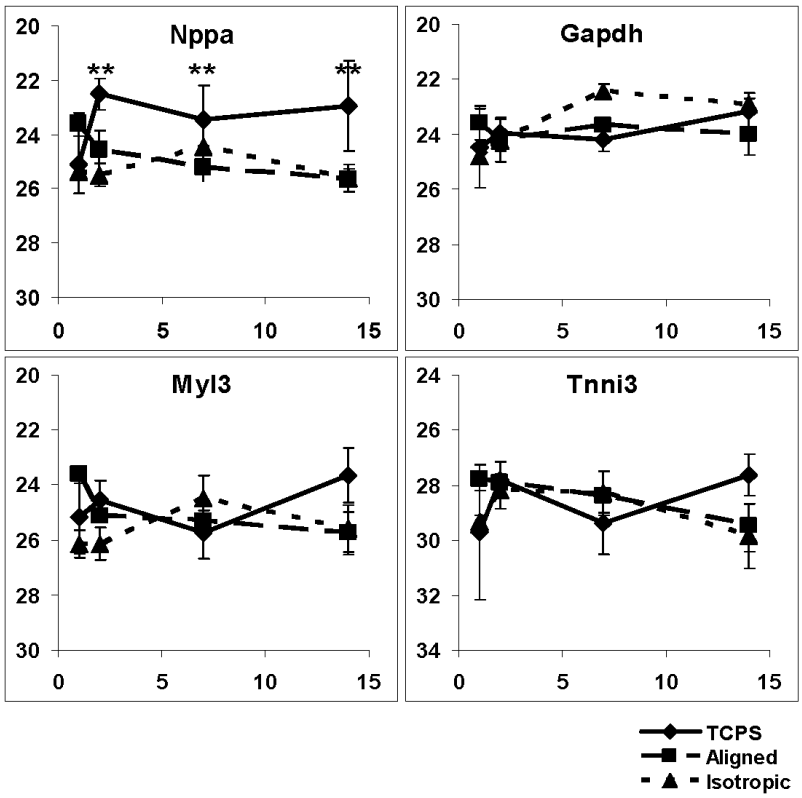

Figure 5. Real time qPCR analysis of gene expression

Steady state mRNA levels for primary cardiac cells cultured for 1, 2, 7, and 14 days are shown. Note that Ct values on the y-axis are in reverse order because a lower Ct indicates higher expression. Asterisks indicate statistically significant differences ($p<0.05$) at the given day based on 2-Way ANOVA with a Tukey-HSD post-hoc test. Nppa expression was found to be significantly elevated in TCPS based cultures over ES-PU cultures. Gapdh, Tnni3, and Myl3 levels were each similar across the different culture types.

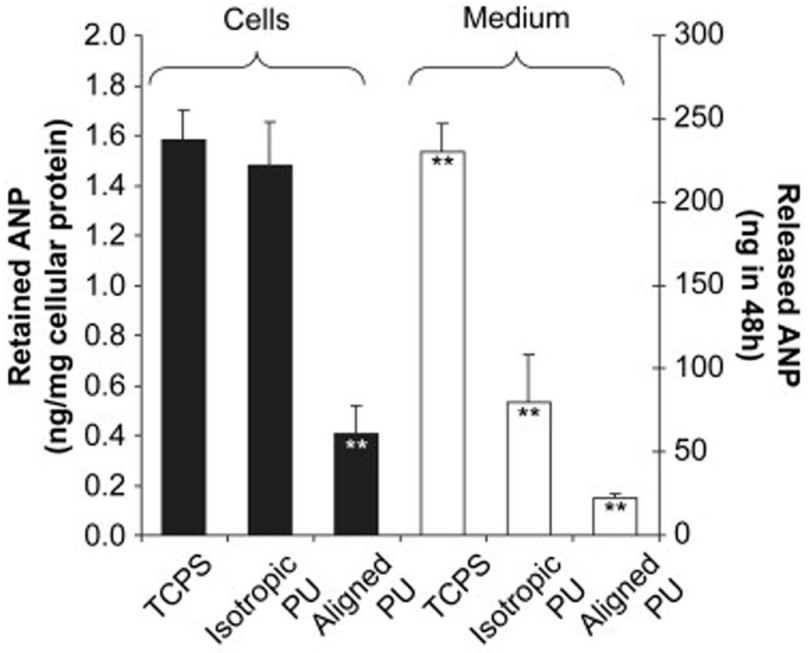

Figure 6. Assessment of immunoreactive ANP

Analysis of ANP levels detected by immunoassay at day 7 of culture shows that cells on aligned ES-PU had lower steady state ANP levels than cells plated on either TCPS or isotropic ES-PU mats ($p < 0.05$ by ANOVA with post-hoc Tukey-HSD) and that cells plated on aligned ES-PU released significantly less ANP in the 48 hours preceding collection than cells on isotropic ES-PU, which released significantly less than cells on TCPS ($p < 0.05$). Data are mean ± SD, n=3. Asterisks denote that a significant difference was found relative to both remaining samples. Note that the data indicate the combined levels of ANP, pro-ANP, and pre-pro-ANP.